



This is a repository copy of *Valence band offsets of $\text{Sc}_x\text{Ga}_{1-x}\text{N}/\text{AlN}$ and $\text{Sc}_x\text{Ga}_{1-x}\text{N}/\text{GaN}$ heterojunctions.*

White Rose Research Online URL for this paper:
<http://eprints.whiterose.ac.uk/103203/>

Version: Accepted Version

Article:

Tsui, H.C.L., Goff, L.E., Palgrave, R.G. et al. (4 more authors) (2016) Valence band offsets of $\text{Sc}_x\text{Ga}_{1-x}\text{N}/\text{AlN}$ and $\text{Sc}_x\text{Ga}_{1-x}\text{N}/\text{GaN}$ heterojunctions. *Journal of Physics D: Applied Physics*, 49 (26). ISSN 0022-3727

<https://doi.org/10.1088/0022-3727/49/26/265110>

Reuse

Unless indicated otherwise, fulltext items are protected by copyright with all rights reserved. The copyright exception in section 29 of the Copyright, Designs and Patents Act 1988 allows the making of a single copy solely for the purpose of non-commercial research or private study within the limits of fair dealing. The publisher or other rights-holder may allow further reproduction and re-use of this version - refer to the White Rose Research Online record for this item. Where records identify the publisher as the copyright holder, users can verify any specific terms of use on the publisher's website.

Takedown

If you consider content in White Rose Research Online to be in breach of UK law, please notify us by emailing eprints@whiterose.ac.uk including the URL of the record and the reason for the withdrawal request.



eprints@whiterose.ac.uk
<https://eprints.whiterose.ac.uk/>

Valence band offsets of $\text{Sc}_x\text{Ga}_{1-x}\text{N}/\text{AlN}$ and $\text{Sc}_x\text{Ga}_{1-x}\text{N}/\text{GaN}$ heterojunctions

H. C. L. Tsui¹, L. E. Goff^{1,2}, R. G. Palgrave³, H. E. Beere², I. Farrer², D. A. Ritchie², M. A. Moram¹

¹Dept. Materials, Imperial College London, Exhibition Road, London SW7 2AZ, UK

²Dept. Physics, University of Cambridge, JJ Thomson Avenue, Cambridge CB3 0HE, UK

³Dept. Chemistry, University College London, 20 Gordon Street, London WC1H 0AJ, UK

Abstract

The valence band offsets of $\text{Sc}_x\text{Ga}_{1-x}\text{N}/\text{AlN}$ heterojunction were measured by X-ray photoelectron spectroscopy (XPS) and were found to increase from 0.42 eV to 0.95 eV as the Sc content x increased from 0 to 0.15. The increase in valence band offset with increasing x is attributed to the corresponding increase in spontaneous polarisation of the wurtzite structure. The $\text{Sc}_x\text{Ga}_{1-x}\text{N}/\text{AlN}$ heterojunction is type I, similar to other III-nitride-based heterojunctions. The results also indicated that a type II staggered heterojunction, which can enhance spatial charge separation, could be formed if $\text{Sc}_x\text{Ga}_{1-x}\text{N}$ is grown on GaN.

Keywords: ScGaN, heterojunction, molecular beam epitaxy, X-ray photoelectron spectroscopy, valence band offset

PACS codes: 78.66.Fd, 79.60.Jv, 81.15.Hi

Introduction

Wurtzite structure III-nitrides and their alloys are used widely in optoelectronics, especially in light emitting diodes (LEDs). By controlling the composition of the nitride alloys, the band gap can be adjusted from 6.2 eV to 0.9 eV, covering the ultraviolet (UV) to infrared wavelength range¹⁻⁴. However, although LEDs emitting in the blue wavelength range have internal quantum efficiencies as high as 90 %, improved device designs are needed in the deep-UV range used for germicidal applications (260 – 280 nm) because the internal quantum efficiencies in this range are currently only 30%⁵⁻⁹. The low efficiencies are due in part to the extended defects which appear within the active light-emitting regions of device heterostructures due to the lattice constant mismatch between layers. The high tensile stresses which typically develop due to the lattice constant and thermal expansion coefficient mismatches between layers within a UV-LED device structure also limit the total device thickness and the variety of structures which can be grown successfully¹⁰⁻¹². Therefore, alternative wurtzite nitrides such as $\text{Sc}_x\text{Ga}_{1-x}\text{N}$ with different lattice parameter – band gap relationships¹³ are of interest to control internal stresses and open up new routes to device design. In this regard, $\text{Sc}_x\text{Ga}_{1-x}\text{N}/\text{AlN}$ heterojunctions are of interest for the active regions of UV light emitters, however the band offsets and the heterojunction type must first be established and confirmed experimentally.

$\text{Sc}_x\text{Ga}_{1-x}\text{N}$ is an alloy between wurtzite GaN and rock-salt ScN, therefore a structural phase transition is expected to occur as the Sc content x increases. $\text{Sc}_x\text{Ga}_{1-x}\text{N}$ films grown using molecular beam epitaxy (MBE) under nitrogen-rich conditions showed a transition from the wurtzite to the cubic structure at approximately $x = 0.17$ ¹⁴ whereas the films grown under metal-rich conditions remained in the wurtzite structure up to $x = 0.26$, consistent with a recent high quality theoretical calculation^{13,15}. Recent data from high quality wurtzite $\text{Sc}_x\text{Ga}_{1-x}\text{N}$

x N films showed that the optical band gap increases with increasing Sc content, consistent with recent theoretical calculations^{13,16}; a decrease in the band gap of $\text{Sc}_x\text{Ga}_{1-x}\text{N}$ with increasing x (as reported previously^{14,17}) only occurs with increasing Sc content in the presence of nanoscale inclusions¹⁶.

The valence band offset (ΔE_v) at a semiconductor interface is an important parameter in designing and modelling quantum well structures and devices^{18–22}. It can be measured by optical spectroscopy (e.g. optical absorption and photoluminescence), electron spectroscopy (e.g. X-ray photoelectron spectroscopy (XPS) and ultraviolet photoelectron spectroscopy (UPS)) and electrical measurement (e.g. I-V and C-V measurements of a device)^{21,22}. Among them, XPS is the most commonly used technique as it allows direct measurement of the valence band edge relative to the Fermi level along with the core level binding energy, whereas simulation and fitting are needed for other techniques^{21–23}. Since the $\text{Sc}_x\text{Ga}_{1-x}\text{N}$ films grown on MOVPE AlN have better crystal quality, the ΔE_v for $\text{Sc}_x\text{Ga}_{1-x}\text{N}/\text{AlN}$ heterojunction is of interest for its potential devices¹⁶. Therefore, this study aims to investigate the influence of Sc to the valence band offsets of the $\text{Sc}_x\text{Ga}_{1-x}\text{N}/\text{AlN}$ heterojunction using XPS.

Experimental

Epitaxial (0001)-oriented $\text{Sc}_x\text{Ga}_{1-x}\text{N}$ thin films were deposited on (0001)-sapphire under metal-rich conditions using molecular beam epitaxy with an RF nitrogen plasma source. The composition of the film was controlled by varying the Sc flux by controlling the effusion cell temperature, while the Ga flux was kept constant. The Sc flux varied between 0 nA and 2 nA, which corresponds to a Sc content x of 0 and 0.15 according to previous Rutherford backscattering measurements¹⁶. The film thicknesses (~ 5 nm and ~ 100 nm) were estimated from the growth rate reported in Ref. 15. X-ray photoelectron spectroscopy (XPS) analysis was performed using a Thermo Scientific K α instrument with monochromated Al K α X-ray sources (1486.6 eV).

Results and discussions

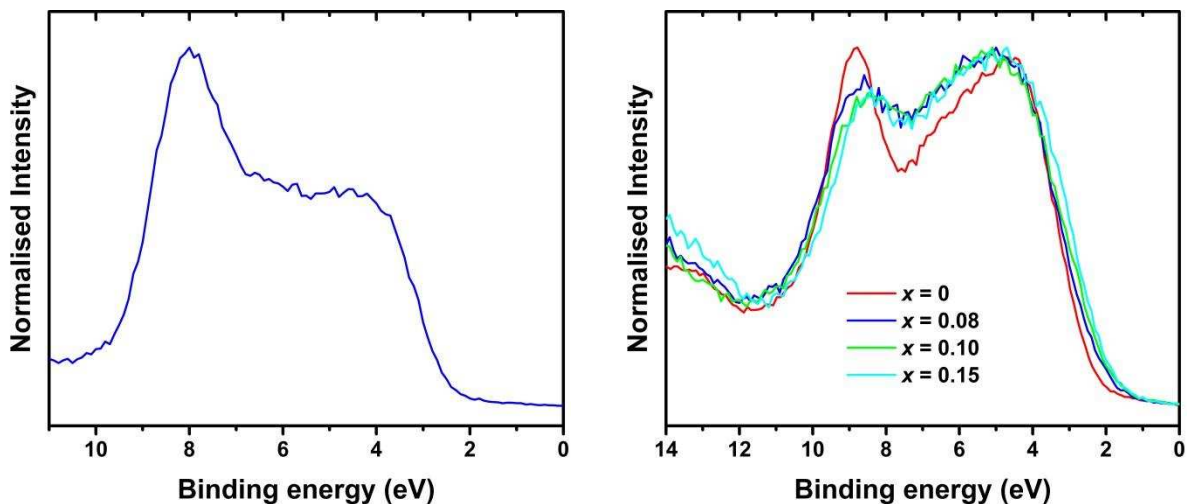


Fig. 1. Valence band spectra for (a) AlN and (b) $\text{Sc}_x\text{Ga}_{1-x}\text{N}$.

The valence band spectra for AlN, GaN and $\text{Sc}_x\text{Ga}_{1-x}\text{N}$ are shown in Fig. 1, where the shape of the spectra of GaN and $\text{Sc}_x\text{Ga}_{1-x}\text{N}$ is similar, with the features at 5 eV and 9 eV corresponding to the p states of Ga^{24–26}. The valence band maximum (VBM) was determined by linearly extrapolating the low binding energy onset of the valence band the spectral

baseline²⁷ and the VBM and the core level energy of the samples are listed in Table I. The valence band offsets of the Sc_xGa_{1-x}N/AlN heterojunction were measured by taking separate photoemission spectra from thick films of AlN and Sc_xGa_{1-x}N and also from a thin film (< 5 nm) of Sc_xGa_{1-x}N on top of AlN. From the thick films of AlN and Sc_xGa_{1-x}N, the binding energies of the VBM (denoted E_{VBM}^{AlN} and E_{VBM}^{ScGaN}) and a core line ($E_{Al\ 2p}^{AlN}$ and $E_{Ga\ 3d}^{ScGaN}$ respectively) were determined. In the thin film, $E_{Al\ 2p}^{ScGaN/AlN}$ and $E_{Ga\ 3d}^{ScGaN/AlN}$, being the binding energies of the Al 2p and Ga 3d core lines, were measured. These were input in Eq. (1), to yield the valence band offsets.

$$\Delta E_v = (E_{Ga\ 3d}^{ScGaN} - E_{VBM}^{ScGaN}) - (E_{Al\ 2p}^{AlN} - E_{VBM}^{AlN}) + (E_{Al\ 2p}^{ScGaN/AlN} - E_{Ga\ 3d}^{ScGaN/AlN}) \quad (1)$$

The valence band offset for GaN/AlN in this experiment was 0.42 ± 0.05 eV, which is consistent with the experimental value of 0.4 eV reported by Rizzi et al. and the theoretical value of 0.44 eV from Nardelli et al.^{28,29}. However, a wide range of valence band offset values have been reported for III-nitride based heterostructures, especially for GaN/AlN where the values range from 0.4 – 1.36 eV³⁰⁻³⁶. The measured valence band maximum is influenced by the surface stoichiometry and defect levels in the GaN, leading to a large range of the measured energy difference between the core level and the valence band maximum. Therefore, the measured valence band offset depends on the growth method, polarity and defect densities of the films^{21,37}. Moreover, the use of different valence band maximum determination methods may contribute to the wide range of reported values^{27,37}.

Sample	Region	Binding energy (eV) (± 0.05)	FWHM
AlN	Al 2p	73.11	1.16
	VBM	2.42	–
GaN			
GaN/AlN	Ga 3d	20.00	1.61
	Al 2p	73.30	1.22
GaN	Ga 3d	20.00	1.34
	VBM	2.20	–
Sc _x Ga _{1-x} N (x = 0.08)			
Sc _x Ga _{1-x} N/AlN	Ga 3d	19.87	1.67
	Al 2p	73.57	1.21
Sc _x Ga _{1-x} N	Ga 3d	19.82	1.68
	VBM	2.07	–
Sc _x Ga _{1-x} N (x = 0.10)			
Sc _x Ga _{1-x} N/AlN	Ga 3d	19.77	1.73
	Al 2p	73.54	1.23
Sc _x Ga _{1-x} N	Ga 3d	19.73	1.71
	VBM	1.92	–
Sc _x Ga _{1-x} N (x = 0.15)			
Sc _x Ga _{1-x} N/AlN	Ga 3d	19.52	1.77
	Al 2p	73.33	1.25
Sc _x Ga _{1-x} N	Ga 3d	19.66	1.69
	VBM	1.83	–

Table I. Binding energy of the core level and valence band maxima (VBM) of Sc_xGa_{1-x}N and AlN.

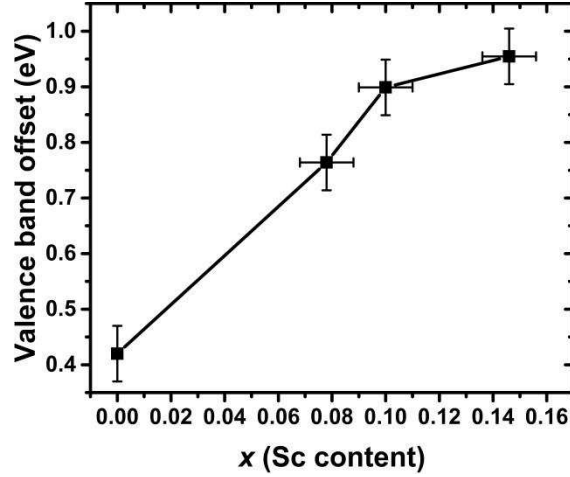


Fig. 2. The valence band offsets of $\text{Sc}_x\text{Ga}_{1-x}\text{N}/\text{AlN}$ heterojunction as a function of Sc content x .

As the Sc content x increased from 0 to 0.15, the valence band offset of the $\text{Sc}_x\text{Ga}_{1-x}\text{N}/\text{AlN}$ heterojunction increased from 0.42 eV to 0.95 eV (Fig. 2). The increase in valence band offsets with increasing x for (0001)-oriented $\text{In}_x\text{Ga}_{1-x}\text{N}/\text{GaN}$ and $\text{Al}_x\text{Ga}_{1-x}\text{N}/\text{GaN}$ heterostructures has been attributed to a strain-induced piezoelectric field oriented along [0001]³⁰. However, as the films grown for this experiment were thicker than the critical thickness suggested by theoretical calculations³⁸, the films appeared to be fully relaxed and thus no strain-induced piezoelectric field contributed to the increase in the valence band offset. On the other hand, the spontaneous polarisation of the wurtzite structure is enhanced by the addition of Sc because of the higher ionicity of the Sc-N bond and the decrease in the c/a lattice parameter ratio with increasing Sc content, as well as the possible contributions from a local internal distortion at the Sc atom site³⁸⁻⁴⁰. The difference in spontaneous polarisation between $\text{Sc}_x\text{Ga}_{1-x}\text{N}$ and AlN leads to charge redistribution at the interface, which is responsible for the increase in valence band offset. It is possible that the doping level would affect the Fermi energy level and thus the measurement of valence band maximum⁴¹, however, since all the GaN and $\text{Sc}_x\text{Ga}_{1-x}\text{N}$ films were grown in the same MBE reactor and under the same conditions, it can be assumed that the doping level for the films were similar.

$$\Delta E_c = (E_g^{\text{AlN}} - E_g^{\text{ScGaN}}) - \Delta E_v \quad (2)$$

The conduction band offset of the heterojunction can be calculated using Eq. (2), where the band gaps of $\text{Sc}_x\text{Ga}_{1-x}\text{N}$ films have been presented in Ref. 16 and the band gap of AlN have been known as 6.2 eV^{13,42}. Therefore, a band alignment diagram can be constructed, as shown in Figure 3. As the band gap of $\text{Sc}_x\text{Ga}_{1-x}\text{N}$ is lower than the band gap of AlN, a type I heterojunction is formed, similar to other III-nitride heterojunctions³⁰. However, Fig. 3 indicates that a type II staggered heterojunction would be formed if $\text{Sc}_x\text{Ga}_{1-x}\text{N}$ is grown on GaN. Type I heterojunction, which is used for light emitting and laser applications, confines electrons and holes on one side of the semiconductor interface leading to greater charge recombination. On the other hand, charges favour separation naturally in type II heterojunction due to the band alignment⁴³⁻⁴⁵, therefore this is an advantage for solar cell⁴⁶⁻⁴⁹ and water splitting applications^{50,51}. The solar cells that used III-nitrides as the active layer have been using the p-i-n structure⁵²⁻⁵⁴, where carrier recombination could lower the efficiency of the solar cell, the formation of $\text{Sc}_x\text{Ga}_{1-x}\text{N}/\text{GaN}$ type II heterojunction may be one solution to this problem.

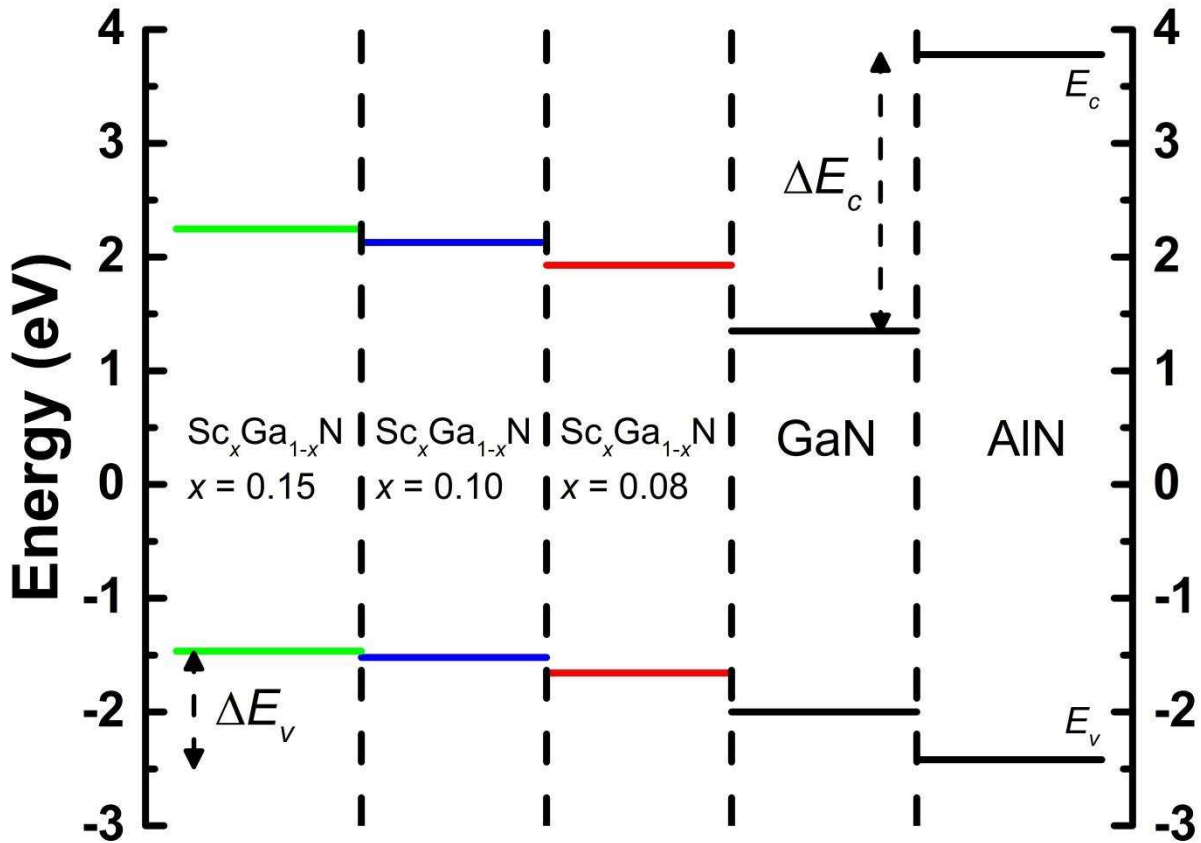


Fig. 3. Band alignments for Sc_xGa_{1-x}N/AlN heterojunctions.

Conclusions

In conclusion, the valence band offset of Sc_xGa_{1-x}N/AlN heterojunction was found to increase as the Sc content increases. This is attributed to the increase in spontaneous polarisation of the wurtzite structure with increasing x. The Sc_xGa_{1-x}N/AlN heterojunction was determined as type I whereas Sc_xGa_{1-x}N/GaN was determined as type II.

Acknowledgements

MAM acknowledges support through a Royal Society University Research Fellowship and through ERC Starting Grant ‘SCOPE’.

References

- ¹H. Morkoc, S. Strite, G. B. Gao, M. E. Lin, B. Sverdlov and M. Burns, *J. Appl. Phys.* **76**, 1363 (1994)
- ²H. Angerer, D. Brunner, F. Freudenberg, O. Ambacher, M. Stutzmann, R. Hopler, T. Metzger, E. Born, G. Dollinger, A. Bergmaier, S. Karsch and H. -J. Korner, *Appl. Phys. Lett.* **71**, 1504 (1997)
- ³S. Nakamura, T. Mukai and M. Senoh, *Appl. Phys. Lett.* **64**, 1687 (1994)
- ⁴V. Yu. Davydov, A. A. Klochikhin, R. P. Seisyan, V. V. Emtsev, S. V. Ivanov, F. Bechstedt, J. Furthmuller, H. Harima, A. V. Mudryi, J. Aderhold, O. Semchinova and J. Graul, *phys. stat. sol. (b)* **229**, R1 (2002)
- ⁵Y. Narukawa, M. Ichikawa, D. Sanga, M. Sano and T. Mukai, *J. Phys. D: Appl. Phys.* **43**, 354002 (2010)

- ⁶S. Nakamura, M. R. Krames, Proc. IEEE **101**, 2211 (2013)
- ⁷S. F. Chichibu, T. Sota, K. Wada, O. Brandt, K. H. Ploog, S. P. DenBaars and S. Nakamura, phys. stat. sol. (a) **183**, 91 (2001)
- ⁸S. F. Chichibu, A. Uedono, T. Onuma, B. A. Haskell, A. Chakraborty, T. Koyama, P. T. Fini, S. Keller, S. P. DenBaars, J. S. Speck, U. K. Mishra, S. Nakamura, S. Yamaguchi, S. Kamiyama, H. Amano, I. Akasaki, J. Han and T. Sota, Nat. Mater. **5**, 810 (2006)
- ⁹Y. Liao, C. Thomidis, C.-k. Kao and T. D. Moustakas, Appl. Phys. Lett. **98**, 081110 (2011)
- ¹⁰A. Khan, K. Balakrishnan and T. Katona, Nat. Photonics **2**, 77 (2008)
- ¹¹I. Akasaki and H. Amano, Jpn. J. Appl. Phys. **36**, 5393 (1997)
- ¹²J. Han, K. E. Waldrip, S. R. Lee, J. J. Figiel, S. J. Hearne, G. A. Petersen and S. M. Myers, Appl. Phys. Lett. **78**, 67 (2001)
- ¹³S. Zhang, D. Holec, W. Y. Fu, C. J. Humphreys and M. A. Moram, J. Appl. Phys. **114**, 133510 (2013)
- ¹⁴C. Constantin, H. Al-Brithen, M. B. Haider, D. Ingram and A. R. Smith, Phys. Rev. B **70**, 193309 (2004)
- ¹⁵H. C. L. Tsui, L. E. Goff, N. P. Barradas, E. Alves, S. Pereira, H. E. Beere, I. Farrer, C. A. Nicoll, D. A. Ritchie and M. A. Moram, phys. stat. sol. (a) **212**, 2837
- ¹⁶H. C. L. Tsui, L. E. Goff, S. K. Rhode, S. Pereira, H. E. Beere, I. Farrer, C. A. Nicoll, D. A. Ritchie and M. A. Moram, Appl. Phys. Lett. **106**, 132103 (2015)
- ¹⁷M. E. Little and M. E. Kordesch, Appl. Phys. Lett. **78**, 2891 (2001)
- ¹⁸I. Vurgaftman and J. R. Meyer, J. Appl. Phys. **94**, 3675 (2003)
- ¹⁹P. D. C. King, T. D. Veal, C. E. Kendrick, L. R. Bailey, S. M. Durbin and C. F. McConville, Phys. Rev. B **78**, 033308 (2008)
- ²⁰C. -L. Wu, C. -H. Shen and S. Gwo, Appl. Phys. Lett. **88**, 032105 (2006)
- ²¹E. T. Yu, J. O. McCaldin and T. C. McGill, Solid State Physics **46**, 1 (1992)
- ²²A. Franciosi and C. G. Van de Walle, Surf. Sci. Rep. **25**, 1 (1996)
- ²³E. A. Kraut, R. W. Grant, J. R. Waldrop and S. P. Kowalczyk, Phys. Rev. Lett. **44**, 1620 (1980); Phys. Rev. B **28**, 1965 (1983)
- ²⁴D. Skuridina, D. V. Dinh, B. Lacroix, P. Ruterana, M. Hoffmann, Z. Sitar, M. Pristovsek, M. Kneissl and P. Vogt, J. Appl. Phys. **114**, 173503 (2013)
- ²⁵M. Kocan, A. Rizzi, H. Luth, S. Keller and U. K. Mishra, phys. stat. sol. (b) **234**, 773 (2002)
- ²⁶P. Lorenz, T. Haensel, R. Gutt, R. J. Koch, J. A. Schaefer and S. Krischok, phys. stat. sol. (b) **247**, 1658 (2010)
- ²⁷S. A. Chambers, T. Droubay, T. C. Kaspar and M. Gutowski, J. Vac. Sci. Technol. B **22**, 2205 (2004)
- ²⁸A. Rizzi, R. Lantier, F. Monti, H. Luth, F. D. Sala, A. D. Carlo and P. Lugli, J. Vac. Sci. Technol. B **17**, 1674 (1998)
- ²⁹M. B. Nardelli, K. Rapcewicz and J. Bernholc, Phys. Rev. B **55**, R7323 (1997)
- ³⁰G. Martin, A. Botchkarev, A. Rockett and H. Morkoc, Appl. Phys. Lett. **68**, 2541 (1996)
- ³¹G. Martin, S. Strite, A. Botchkarev, A. Agarwal, A. Rockett, H. Morkoc, W. R. L. Lambrecht and B. Segall, Appl. Phys. Lett. **65**, 610 (1994)
- ³²J. R. Waldrop and R. W. Grant, Appl. Phys. Lett. **68**, 2879 (1996)
- ³³S. W. King, C. Ronning, R. F. Davis, M. C. Benjamin and R. J. Nemanich, J. Appl. Phys. **84**, 2086 (1998)
- ³⁴E. A. Albanesi, W. R. L. Lambrecht and B. Segall, J. Vac. Sci. Technol. B **12**, 2470 (1994)
- ³⁵S. Satpathy, Z. S. Popovic and W. C. Mitchel, J. Appl. Phys. **95**, 5597 (2004)
- ³⁶F. Bernardini and V. Fiorentini, Phys. Rev. B **57**, R9427 (1998)
- ³⁷S. W. King, C. Ronning, R. F. Davis, M. C. Benjamin and R. J. Nemanich, J. Appl. Phys. **84**, 2086 (1998)
- ³⁸S. Zhang, W. Y. Fu, D. Holec, C. J. Humphreys and M. A. Moram, J. Appl. Phys. **114**,

- 243516 (2013)
- ³⁹F. Tasnadi, B. Alling, C. Hoglund, G. Wingqvist, J. Birch, L. Hultman and I. A. Abrikosov, *Phys. Rev. Lett.* **104**, 137601 (2010)
- ⁴⁰M. A. Caro, S. Zhang, T. Riekkinen, M. Ylilammi, M. A. Moram, O. Lopez-Acevedo, J. Molarius and T. Laurila, *J. Phys.: Condens. Matter* **27**, 279602 (2015)
- ⁴¹W.-X. Ni, J. Knall and G. V. Hansson, *Phys. Rev. B* **36**, 7744 (1987)
- ⁴²W. M. Yim, E. J. Stofko, P. J. Zanzucchi, J. I. Pankove, M. Ettenberg and S. L. Gilbert, *J. Appl. Phys.* **44**, 292 (1973)
- ⁴³Z. I. Alferov, *Rev. Mod. Phys.* **73**, 767 (2001)
- ⁴⁴M. P. Mikhailova and A. N. Titkov, *Semicond. Sci. Technol.* **9**, 1279 (1994)
- ⁴⁵M. Sacilotti, B. Champagnon, P. Abraham, Y. Monteil and J. Bouix, *J. Lumin.* **57**, 33 (1993)
- ⁴⁶Y. Tomita, T. Kawai and Y. Hatanaka, *Jpn. J. Appl. Phys.* **32**, 1923 (1993)
- ⁴⁷E. C. Garnett, M. L. Brongersma, Y. Cui and M. D. McGehee, *Annu. Rev. Mater. Res.* **41**, 269 (2011)
- ⁴⁸M.-L. Tsai, S.-H. Su, J.-K. Chang, D.-S. Tsai, C.-H. Chen, C.-I. Wu, L.-J. Li, L.-J. Chen and J.-H. He, *ACS Nano* **8**, 8317 (2014)
- ⁴⁹J. Schrieer, D. O. Demchenko, L.-W. Wang and A. P. Alivisatos, *Nano Lett.* **7**, 2377 (2007)
- ⁵⁰J. Kang, S. Tongay, J. Zhou, J. Li and J. Wu, *Appl. Phys. Lett.* **102**, 012111 (2013)
- ⁵¹S. J. A. Moniz, S. A. Shevlin, D. J. Martin, Z.-X. Guo and J. Tang, *Energy Environ. Sci.* **8**, 731 (2015)
- ⁵²O. Jani, I. Ferguson, C. Honsberg and S. Kurtz, *Appl. Phys. Lett.* **91**, 132117 (2007)
- ⁵³R. Dahal, B. Pantha, J. Li, J. Y. Lin and H. X. Jiang, *Appl. Phys. Lett.* **94**, 063505 (2009)
- ⁵⁴E. Matioli, C. Neufeld, M. Iza, S. C. Cruz, A. A. Al-Heji, X. Chen, R. M. Farrell, S. Keller, S. DenBaars, U. Mishra, S. Nakamura, J. Speck and C. Weisbuch, *Appl. Phys. Lett.* **98**, 021102 (2011)